Supporting Information

Autoxidation of Siphonochilone in Processed Rhizomes and Stored Powders of *Siphonochilus aethiopicus* (Schweinf.) B.L. Burtt

Félix Katele Zongwe, Jules Tshishimbi Muya, Raphael Mutimana, Mudogo Virima, Muzomwe Mayaliwa, Hoeil Chung, and Vinesh Maharaj*

Supporting information

General experimental procedure.

NMR data were recorded on a Bruker Avance III 400 MHz magnet operating at 400.21 MHz for ^{1}H and 100.64 MHz for ^{13}C. Chemical shifts are reported in ppm, *J* coupling constants in hertz (Hz) and the multiplicity of ^{1}H peaks are denoted with corresponding letters in italic (e.g., *s*: singlet, *d*: doublet, *dd*: doublet of doublets, *t*: triplet, *m*: multiplet, etc.). Ultra performance liquid chromatography experiments were accomplished with an Acquity UPLC, coupled to a Waters Synapt G2 QTOF mass spectrometer using an electrospray ionization (ESI) technique operating in positive or negative modes, and were performed with an Acquity UPLC BEH C18 1.7 µm 2.1 x 100 mm column from Waters. A linear gradient system was used for the UPLC separation, consisting of 1% formic acid in deionized water (Solvent A) and 1% formic acid in acetonitrile (solvent B) with a constant flow rate of 0.30 mL min^{-1}: 0 to 2 min (95% A: 5% B), 2 to 30 min (1% A: 99% B), 30 to 40 min (1% A: 99% B), 40 to 45 min (95% A: 5% B), 45 to 60 min (95% A: 5% B). TOF MS data were acquired in the range of 100-1200 atomic mass units (amu) for a scan time of 0.5 seconds, using the electrospray positive mode (ES+). The cone voltage was ramped from 20 to 40 V. LC MS and MS/MS chromatograms were processed and visualized using the MassLynx v.4.1 software and further improved with CorelDraw X7. Thin layer chromatography was performed on Merck silica gel 60 F_{254} plates which were later visualized with either iodine or 254 and 366 nm UV lights; column chromatography was performed on Merck silica gel 60 (0.063-0.20 mm). X-ray diffraction experiments were realized on a Bruker D8 Venture diffractometer, using a Cu Kα source and a Photon 100 detector.

Drying, extraction and isolation of compounds 1 and 3.

Fresh African ginger rhizomes were received from the department of Enterprise Creation and Development (ECD) based at the Council for Scientific and Industrial Research (CSIR). The fresh rhizomes were harvested in Septembre 2014 from the cultivation site in Giyani, Limpopo Province, South Africa, and identified as *Siphonochilus aethiopicus* (Schweinf.) B.L. Burtt by ECD. 250g of fresh rhizomes were cut into 1-2 mm slices and portions were left to dry in a fume hood for approximately 11 days. The dried slices were subsequently grinded, and part of the resulting powder was stored in transparent plastic bags at room temperature for about nine months. Extracts for UPLC QTOF MS ES+ analysis were prepared by separately stirring overnight 10g of the crushed fresh rhizomes, powdered and processed plants and nine months stored powders in 100 ml of n-hexane/dicholoromethane (1:1) followed by filtration and evaporation of the solvent using a Büchi rotary evaporator. For the fresh rhizomes, the filtrate was concentrated with a rotary evaporator and dried out in a fume hood. Isolation of Siphonochilone (**1**) was done through silica gel column chromatography of the crude extract (0.565 g) prepared from the crushed fresh rhizomes. The extract was fractionated by gradient elution, starting with acetone/DCM (3:17) and progressively increasing up to acetone/DCM (2:3). A total of 21 fractions were collected, analyzed by TLC and grouped accordingly. TLC plates were developed with acetone/DCM (1:9) and alternately visualized with iodine and both 254 and 366 nm UV lights. 8 spots were revealed with the following R_f values 0.93, 0.86 (most intense spot), 0.78, 0.67, 0.58, 0.53, 0.22 and 0.16. Fractions 5 to 8, which displayed the most spot on the TLC plates, were combined and dried out to afford F1. F1 was resolved with silica gel column chromatography using an isocratic elution with EtOAc/n-hexane (3:17); and 80 sub-fractions were obtained. The sub-fractions were TLC analyzed using

EtOAc/hexane (3:7), and the visualization of the plates was done using UV lamps and an iodine chamber. The sub-fractions 62 to 79 displayed a very intense spot with the R_f value of 0.68 and were accordingly mixed and concentrated with a Büchi rotary evaporator to afford F1a. Overnight crystallization of F1a gave Siphonochilone (**1)** as a colorless crystalline compound. Isolation of the lactone (**3**) was achieved in two steps using the n-hexane/dicholoromethane (1:1) extract (0.554 g) prepared from the stored powder. The first fractionation was done on a silica gel column using a gradient of acetone/DCM (from 3:17 to 2:3). 21 fractions were obtained and based on the TLC similarities, fractions 12-21 were mixed and the solvent evaporated. The combined fractions were further fractionated using silica gel column chromatography and an isocratic elution with the mixture acetone/EtOAc/n-hexane (2:3:5). A total of 80 sub-fractions were collected and analyzed by TLC using acetone/EtOAc/n-hexane (2:3:5). The plates were visualized with an iodine chamber. Based on TLC profiles, sub-fractions 12 to 37 were pooled and concentrated using a Büchi rotary evaporator, resulting in the lactone derivative **3** as colorless crystals.

Computational method

The initial geometries of **1** and **3** were built from the crystallographic data and optimized at B3LYP and MP2 theoretical levels, using 6-31+G(d,p) and 6-311+G(2d,p) basis sets. To ensure that the optimized geometries correspond to true minima on the potential energy surface, harmonic vibrational analysis was carried out at B3LYP/6-311+G(2d,p) level. The chemical shifts of **1** and **3** refer to C (182.4656) and H (31.8821) shielding of TMS and the 1H-H spin-spin coupling constants were computed, at B3LYP with 6-311+G(2d,p) in dichloromethane for **1** and chloroform for **3**, employing the polarizable continuum model (PCM). The optimized geometric structures and the spectroscopic data of **1** and **3** were compared with available experimental data. To predict reactivity of **1** and **3** frontier molecular orbitals were analyzed at MP2/6-31+G(d,p) because B3LYP has tendency to underestimate the HOMO-LUMO energy gap. All the calculations were obtained using Gaussian 09D.[1] For visualisation purpose ChemDraw, Gaussview5[2] and Chemcraft 4.3 were used.

Isolation of peak F from the stored powder of African ginger rhizomes:

The comparison between the UPLC-qTOF-MS profile of siphonochilone after decomposition (chromatogram a) and that of the stored powder (chromatogram b) established the identity of peaks E′ and F′ to be the same as that of E and F. Peaks are labelled with respect to Figure 6 in the article. Peak F was isolated from the stored powder using silica gel column chromatography.

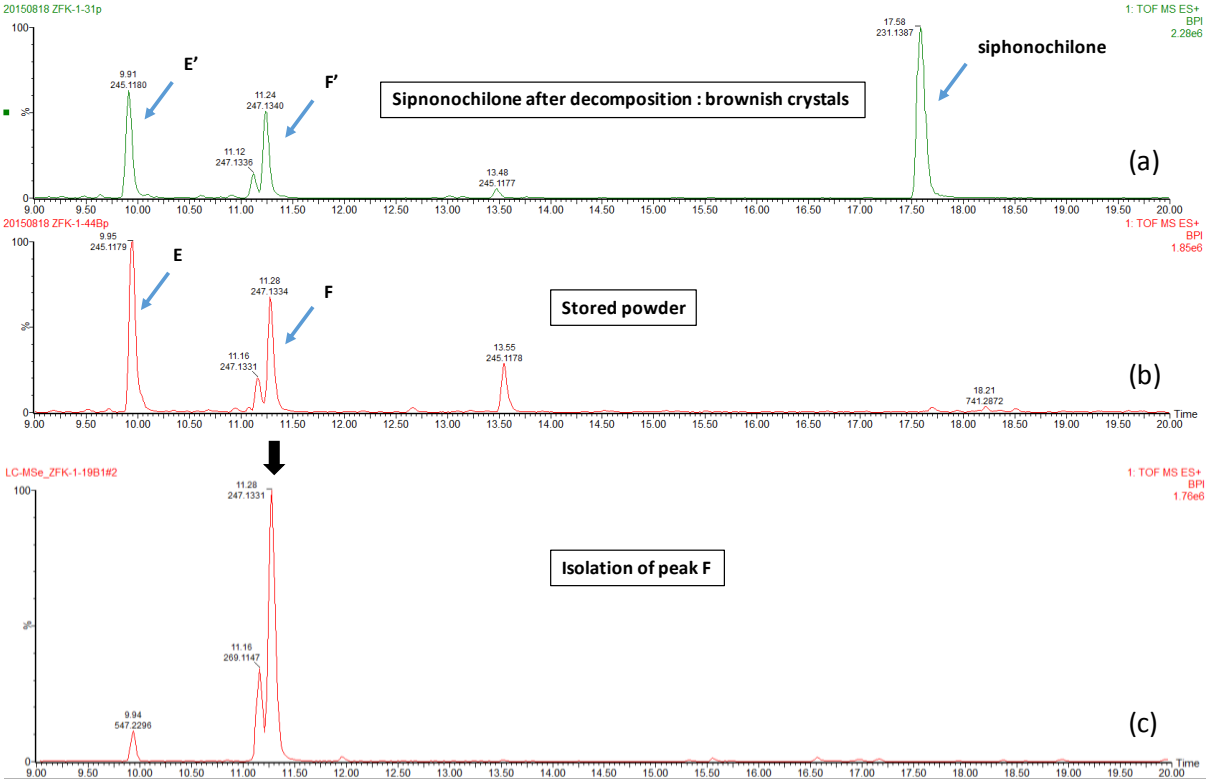

Figure 1: UPLC QTOF MS chromatograms of siphonochilone after decomposition (a), store powder (b) and the isolated fraction containing F as the major peak.

Isolation of peak F: 1.216 g of the n-hexane/DCM (1:1) extract prepared from the stored powder was subjected to silica gel column chromatography using a gradient of n-hexane and EtOAc (0 - 50% EtOAc). 340 fractions of about 10 ml each were collected. Based on their TLC profile, fractions 288-320 were grouped and dried out using a Buchi rotavap. The yellow oil obtained was analysed with help of UPLC-qTOF-MS (Figure 1c) and further subjected to 1 and 2D NMR experiments (Figure 2-14). Conclusive investigation of the NMR data allowed identification of peak F as compound **4** within the isolated mixture.

NMR data of the isolated peak F and comparison with reported data:

Table 1: comparison between ^{1}H and ^{13}C data (in $CDCl_3$) with chemical shifts in literature (lit.)[#]* and B3LYP/6-311+G(2d,p) predicted data (PCM chloroform).

position	δ_H (*J* in Hz)	δ_H B3LYP/6-311+G(2d,p)	δ_H Lit. (*J* in Hz)	δ_C	δ_C B3LYP/6-311+G(2d,p)	δ_C Lit.
2				174.3	185.1	174.2
3				120.7	129.9	119.7
3a				159.7	173.3	161.0
4	2.94 *dd* (14.2, 4.3)	3.1	3.03 *dd* (14.3, 4.8)	25.6	28.9	25.2
	2.21 *m*	2.3	2.31 *dd* (14.3, 12.0)			
4a	1.6 *ddd* (12.9, 10.0, 4.3)	1.5	1.64 *dd* (13.8, 4.2)	48.3	54.0	48.1
5	2.4 *m*	2.6	2.5 *tq* (7.2, 2.4)	34.1	39.7	36.4
6	6.63 *dd* (10.0, 2.0)	7.0	6.76 *dd* (10.2, 2.4)	153.4	167.1	154.5
7	5.86 *dd* (10.0, 2.8)	6.2	5.84 *dd* (10.2, 2.4)	126.2	133.5	125.3
8				201.7	216.9	202.2
8a				44.9	49.9	44.9
9	2.76 *dd* (12.9, 6.1)	2.9	2.66 *dd* (12.9, 6.0)	39.7	44.4	39.6
	1.13 *d* (12.9)	1.0	1.63 *dd* (12.9, 4.2)			
9a	4.78 *dd* (12.0, 6.2)	4.9	4.90 *dd* (16.0, 6.6)	77.9	83.5	77.8
3-Me	1.78 *t* (1.7)	1.8	1.78 *d* (1.2)	8.3	9.1	7.4
5-Me	1.21 *d* (7.3)	1.5	1.21 *d* (7.2)	18.1	18.5	17.3
8a-Me	1.18 *s*	1.2	1.31 s	15.8	16.8	15.3

[#] C.A. Lategan, W.E. Campbell, T. Seaman, P.J. Smith, *J. Ethnopharmacol.* **2009**, *121*, 92-97.
*The literature does not mention the solvent that was used for the acquisition of the NMR data.

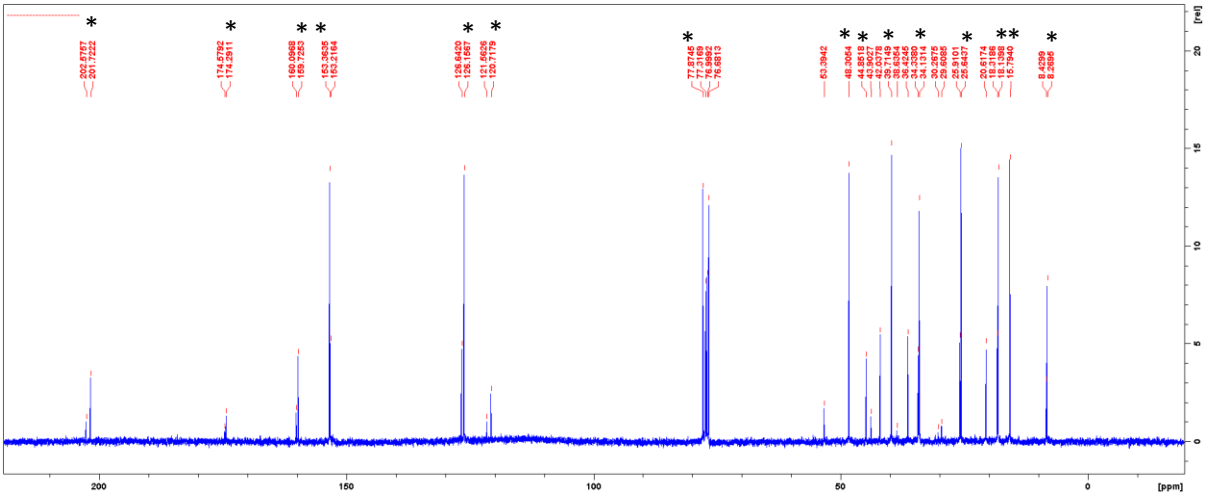

Figure 2: ^{13}C NMR of the isolated fraction with F as the major peak. * indicates the ^{13}C signals allocated to compounds **4** in the isolated mixture.

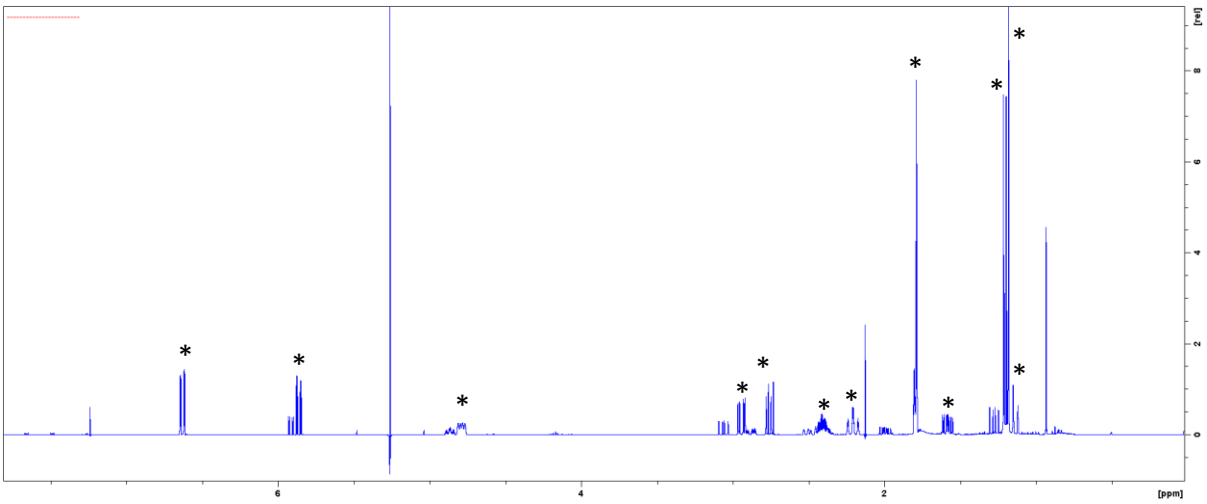

Figure 3: ^{1}H NMR of the isolated fraction with F as the major peak. * indicates the ^{1}H signals allocated to compounds **4** in the isolated mixture.

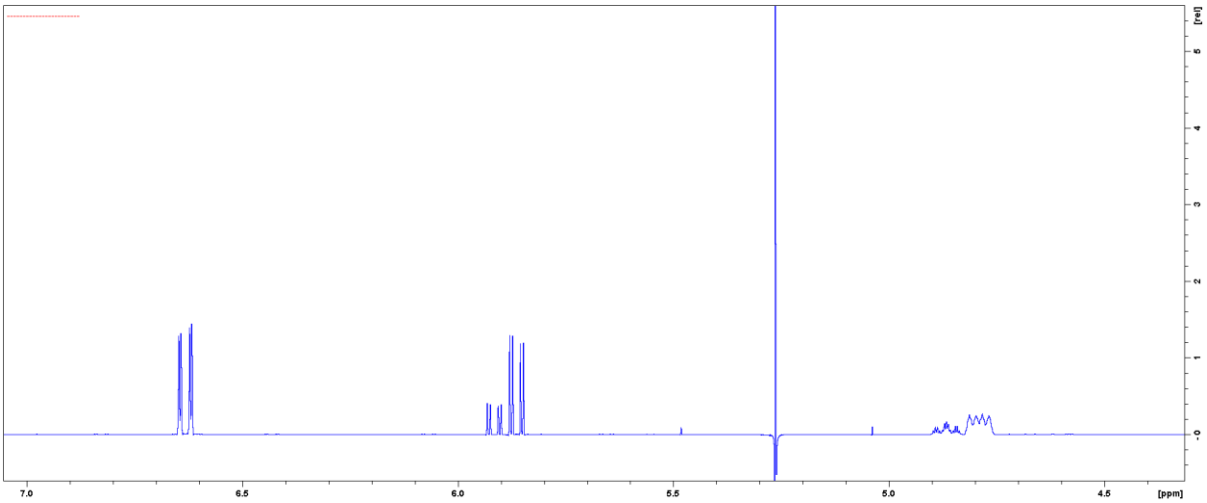

Figure 4: ^{1}H NMR of the isolated fraction with F as the major peak. From 7 to 4 ppm.

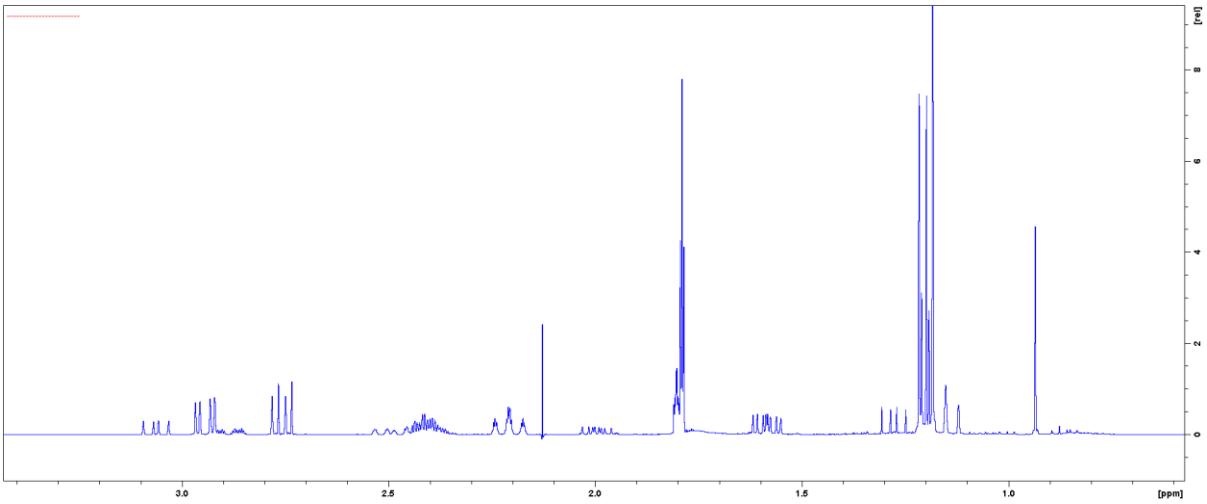

Figure 5: ^{1}H NMR of the isolated fraction with F as the major peak. From 4 to 0 ppm.

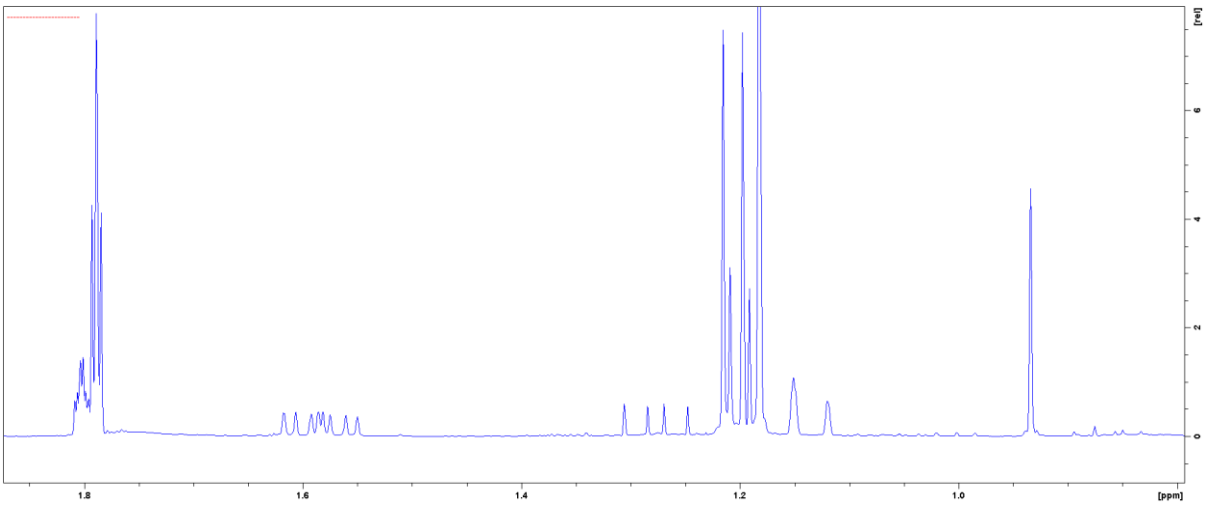

Figure 6: ^{1}H NMR of the isolated fraction with F as the major peak. From 1.8 to 0 ppm.

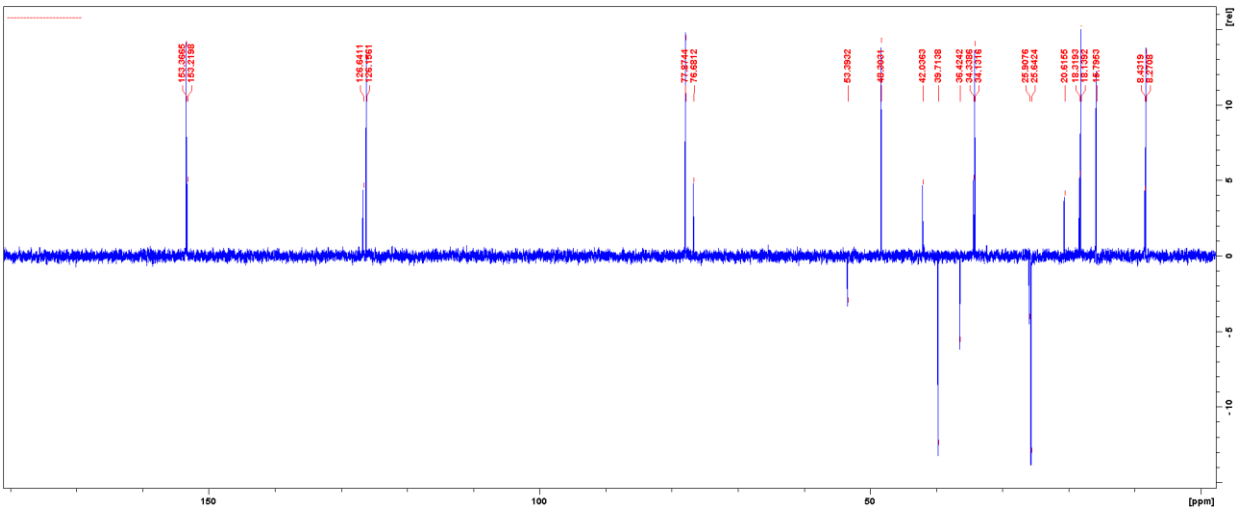

Figure 7: DEPT-135 of the isolated fraction with F as the major peak.

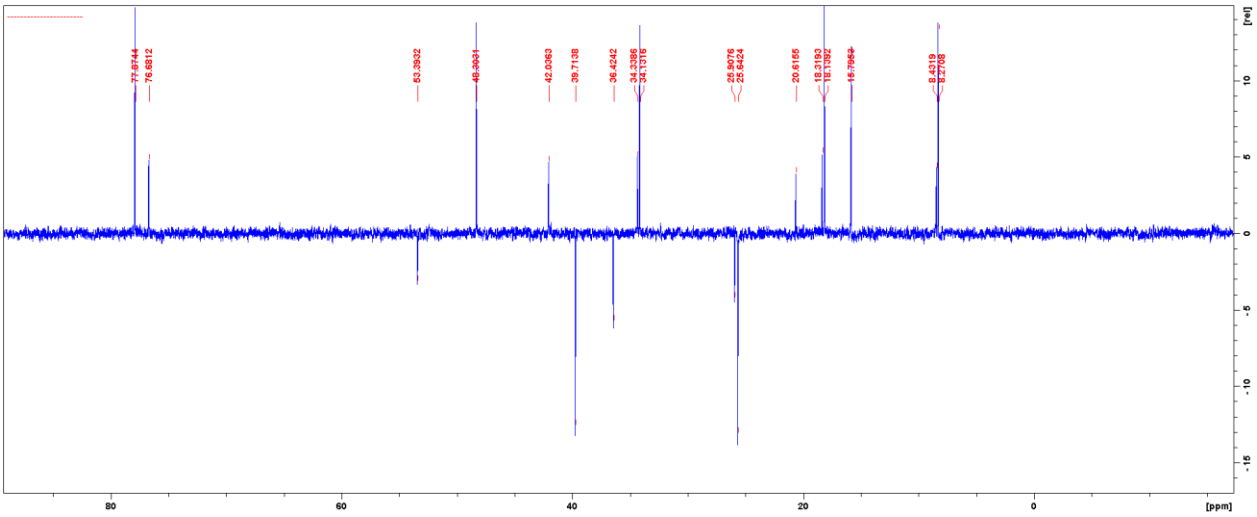

Figure 8: DEPT-135 of the isolated fraction with F as the major peak.

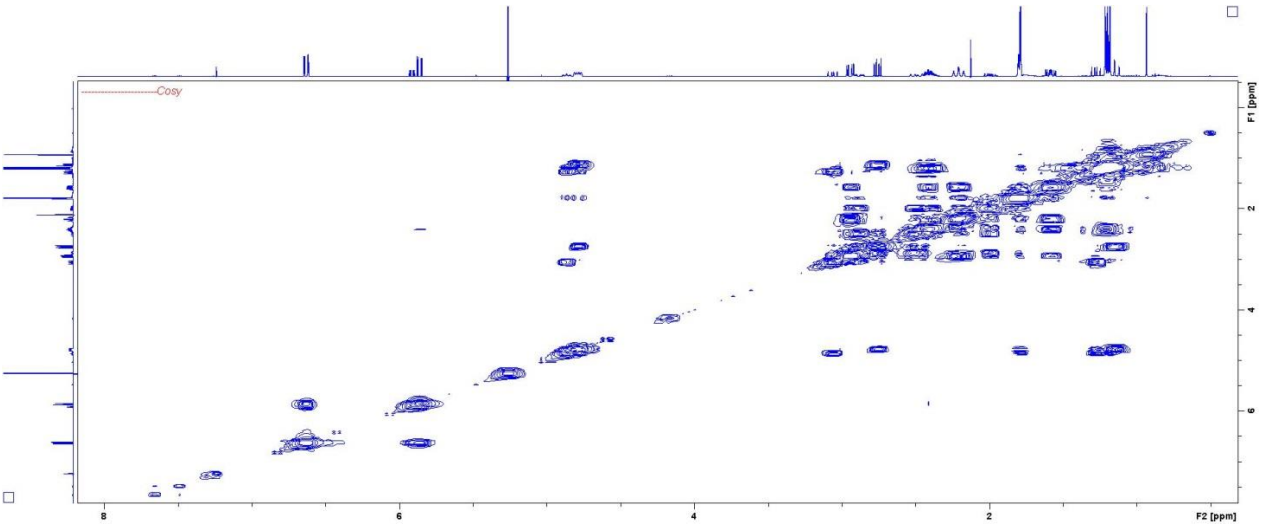

Figure 9: COSY of the isolated fraction with F as the major peak.

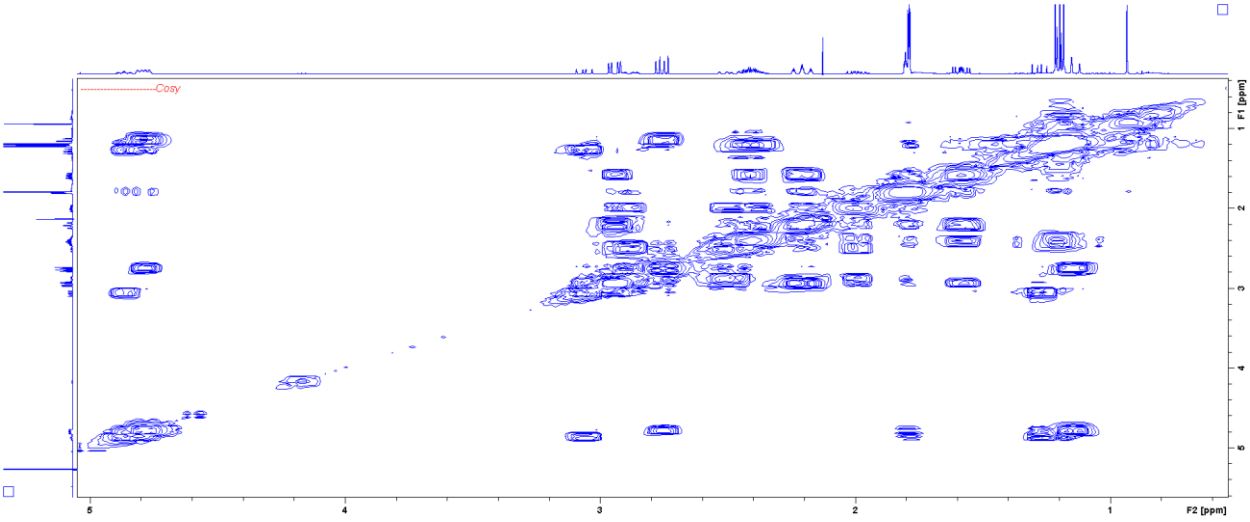

Figure 10: COSY of the isolated fraction with F as the major peak.

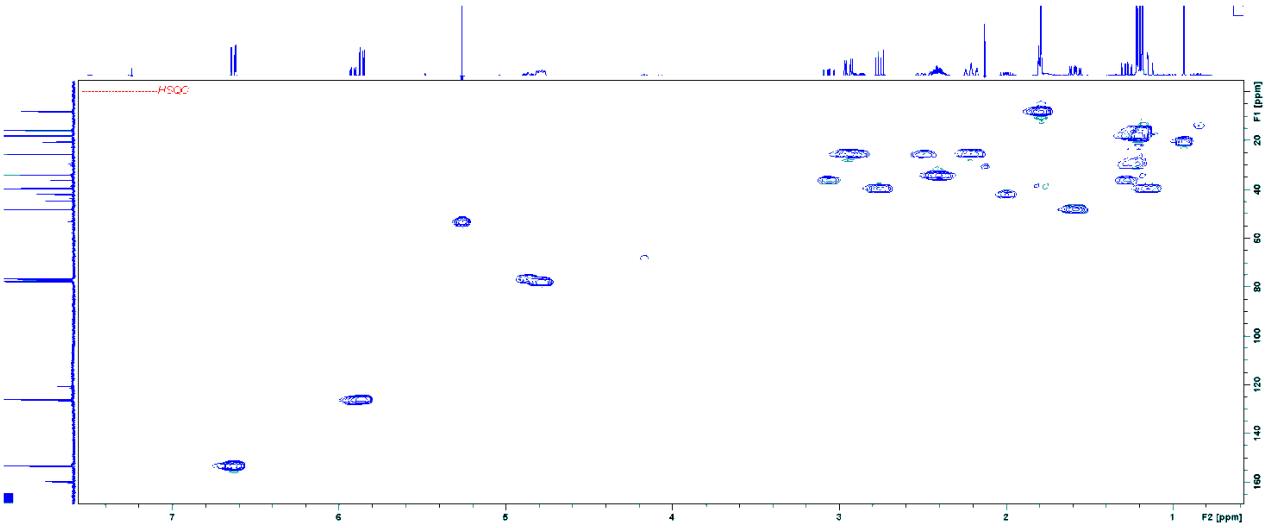

Figure 11: HSQC of the isolated fraction with F as the major peak.

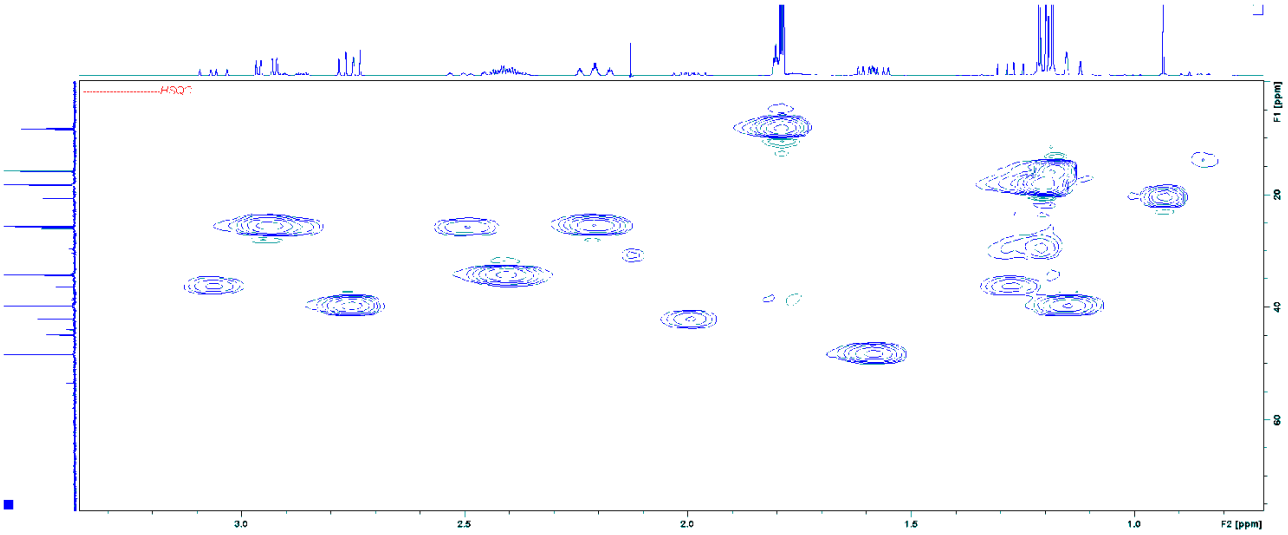

Figure 12: HSQC of the isolated fraction with F as the major peak.

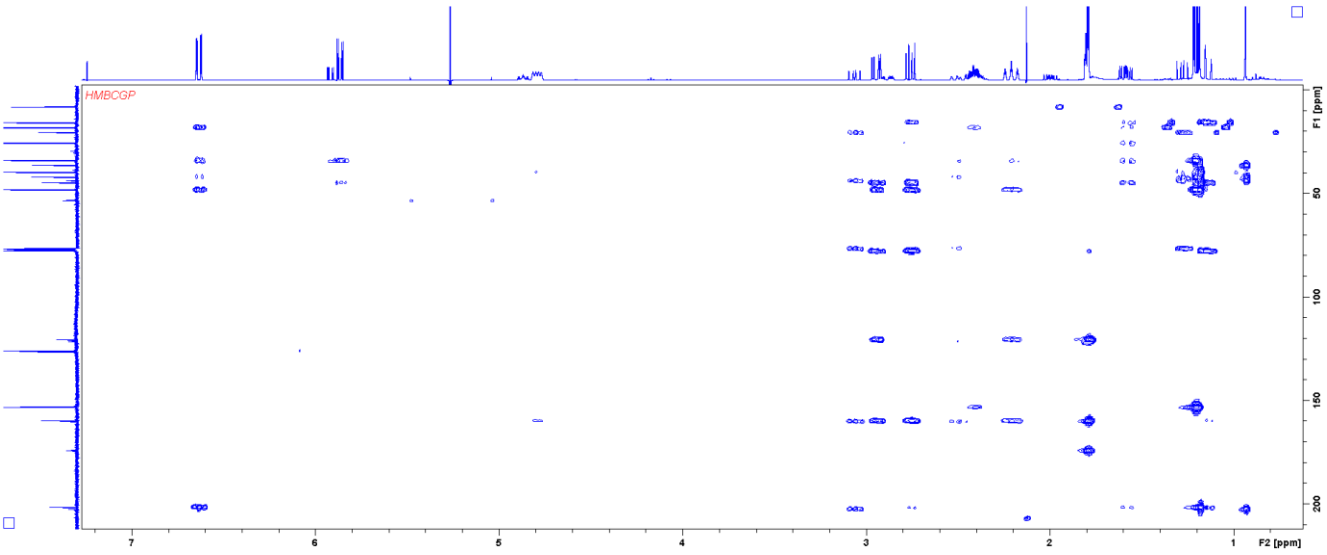

Figure 13: HMBC of the isolated fraction with F as the major peak.

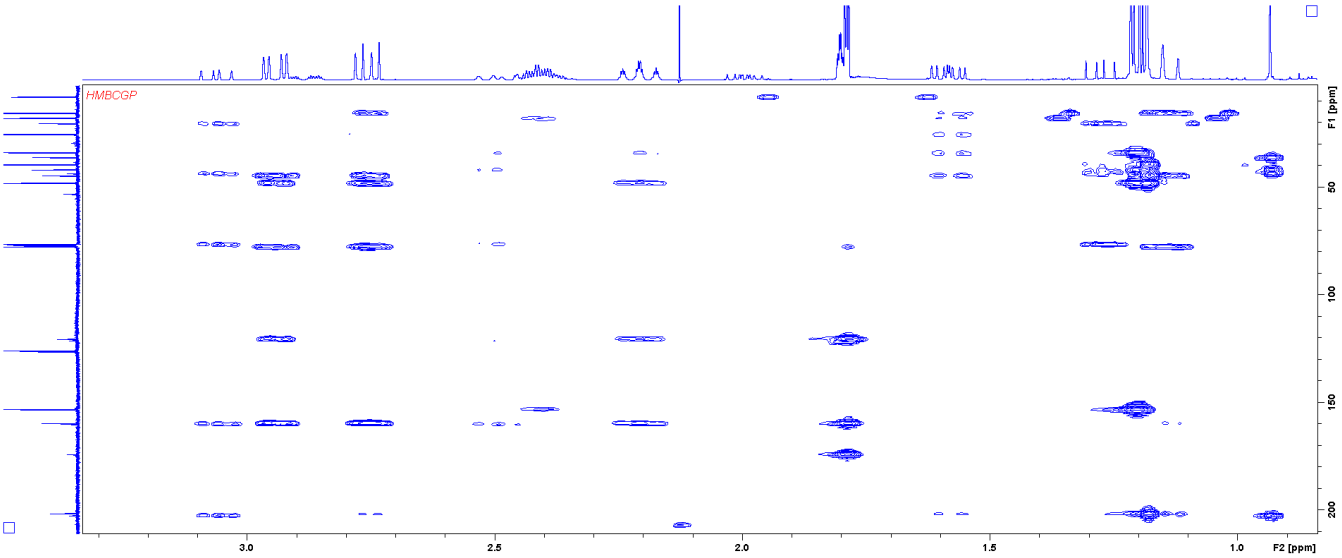

Figure 14: HMBC of the isolated fraction with F as the major peak.

References

[1] M. J. Frisch, G. W. Trucks, H. B. Schlegel, G. E. Scuseria, M. A. Robb, J. R. Cheeseman, G. Scalmani, V. Barone, B. Mennucci, G. A. Petersson, H. Nakatsuji, M. Caricato, X. Li, H. P. Hratchian, A. F. Izmaylov, J. Bloino, G. Zheng, J. L. Sonnenberg, M. Hada, M. Ehara, K. Toyota, R. Fukuda, J. Hasegawa, M. Ishida, T. Nakajima, Y. Honda, O. Kitao, H. Nakai, T. Vreven, J. A. Montgomery, Jr., J. E. Peralta, F. Ogliaro, M. Bearpark, J. J. Heyd, E. Brothers, K. N. Kudin, V. N. Staroverov, R. Kobayashi, J. Normand, K. Raghavachari, A. Rendell, J. C. Burant, S. S. Iyengar, J. Tomasi, M. Cossi, N. Rega, J. M. Millam, M. Klene, J. E. Knox, J. B. Cross, V. Bakken, C. Adamo, J. Jaramillo, R. Gomperts, R. E. Stratmann, O. Yazyev, A. J. Austin, R. Cammi, C. Pomelli, J. W. Ochterski, R. L. Martin, K. Morokuma, V. G. Zakrzewski, G. A. Voth, P. Salvador, J. J. Dannenberg, S. Dapprich, A. D. Daniels, Ö. Farkas, J. B. Foresman, J. V. Ortiz, J. Cioslowski, and D. J. Fox, Gaussian 09, Revision D.01, Gaussian, Inc., Wallingford CT, **2009**.

[2] R. Dennington, T. Keith, J. Millan, GaussView, version 5.0.8, Semichem Inc., Shawnee Mission KS, **2009**.